



ELSEVIER

Journal of Crystal Growth 211 (2000) 295–301

JOURNAL OF  
**CRYSTAL  
GROWTH**

www.elsevier.nl/locate/jcrysgr

# Flux growth and characterization of $\text{Cr}^{4+} : \text{Ca}_2\text{GeO}_4$ crystals as a new near infrared tunable laser material

A.B. Bykov<sup>a,b,\*</sup>, V. Petricevic<sup>a,b</sup>, J. Steiner<sup>c</sup>, Di Yao<sup>d</sup>, L.L. Isaacs<sup>d</sup>,  
M.R. Kokta<sup>e</sup>, R.R. Alfano<sup>a,b</sup>

<sup>a</sup>*Institute for Ultrafast Spectroscopy and Lasers, New York State Center for Advanced Technology for Ultrafast Photonic Materials and Applications, New York, NY 10031, USA*

<sup>b</sup>*Department of Physics, City College and Graduate School, City University of New York, New York, NY 10031, USA*

<sup>c</sup>*Department of Earth and Atmospheric Science, New York, NY 10031 USA*

<sup>d</sup>*Department of Chemical Engineering, New York, NY 10031, USA*

<sup>e</sup>*Bicron Crystal Products, Washougal, WA 98671, USA*

## Abstract

$\text{Cr}^{4+} : \text{Ca}_2\text{GeO}_4$  crystals were grown by pulling technique from  $\text{CaF}_2$ -based solution. RF-heated Czochralski equipment designed for conventional growth procedure from a melt was employed. Stable growth conditions without constitutional supercooling have been created for the pulling rate up to 0.25 mm/h. Only  $\text{Cr}^{4+}$ -substitution took place in the  $\text{Ca}_2\text{GeO}_4$  crystal sites whether the growth atmosphere was nitrogen or air. © 2000 Elsevier Science B.V. All rights reserved.

PACS: 42.70.Hj; 81.10.Dn; 78.20. – e

Keywords: Calcium germanate ( $\text{Ca}_2\text{GeO}_4$ ); Olivine;  $\text{Cr}^{4+}$ -doped lasers; Flux growth; Czochralski method

## 1. Introduction

The development of tunable solid state lasers based on the  $\text{Cr}^{4+}$ -ion began in 1988 with forsterite,  $\text{Mg}_2\text{SiO}_4 : \text{Cr}$  [1]. It was rapidly extended to other crystalline media, such as  $\text{Cr}^{4+}$ -doped  $\text{Y}_3\text{Al}_5\text{O}_{12}$ ,  $\text{Y}_2\text{SiO}_5$ ,  $\text{Y}_3\text{Sc}_x\text{Al}_{5-x}\text{O}_{12}$  [2–4]. The  $\text{Cr}^{4+}$ -ions in tetrahedral coordination proved to be very interesting for the realization of room temper-

ature tunable solid-state laser in the spectral range between 1.1–2  $\mu\text{m}$ . Since the identification of  $\text{Cr}^{4+}$  laser centers in forsterite, synthesis and spectroscopic studies of numerous  $\text{Cr}^{4+}$ -doped olivine-like silicates and germanates have been carried out. It was shown [5,6] that  $\text{Cr}^{4+}$ -doped  $\text{Ca}_2\text{SiO}_4$ ,  $\text{Mg}_2\text{GeO}_4$ ,  $(\text{Ca},\text{Mg})_2\text{GeO}_4$ , and  $\text{Ca}_2\text{GeO}_4$ , all with olivine-type crystal structure are among the few materials that exhibit strong emission in near IR-region. Unfortunately, all silicates and germanates belonging to olivine-type structure family (except forsterite) are characterized by complicated polymorphism and/or incongruent melting point that create difficulties for single crystal preparation.

\* Corresponding author. Department of Physics, City College and Graduate School, City University of New York, New York, NY 10031, USA. Fax: +1-212-650-5530.

E-mail address: bykov@scisun.sei.cuny.cuny.edu (A.B. Bykov)

As a result, only Cr-doped forsterite has been successfully grown by Czochralski technique and fully characterized as IR-laser material. All other silicates and germanates of olivine structure were taken out of consideration as potential laser materials due to unfavorable crystal-growth properties. The extremely strong luminescence of  $\text{Cr}^{4+}$  in the above-mentioned olivine-like materials [7] was the main reason to consider other crystal growth techniques for the growth of these materials. Our attention was focused on single crystal preparation of  $\text{Cr}^{4+} : \text{Ca}_2\text{GeO}_4$ , tuning laser emission of which is expected to cover the important optical communication eye safe wavelength range of 1.3–1.6  $\mu\text{m}$ .

According to Shirvinskaya [8], two modifications ( $\alpha$  and  $\gamma$ ) are known for  $\text{Ca}_2\text{GeO}_4$ . The reversible transformation  $\alpha$ - $\gamma$  occurs at 1453°C. Low-temperature  $\gamma$  -  $\text{Ca}_2\text{GeO}_4$  phase is isostructural with forsterite ( $\text{Mg}_2\text{SiO}_4$ ) and belongs to olivine-type structure with the space group Pbnm. The lattice parameters of  $\text{Ca}_2\text{GeO}_4$  are  $a = 5.240 \text{ \AA}$ ,  $b = 11.400 \text{ \AA}$ , and  $c = 6.790 \text{ \AA}$ . Therefore, crystal growth process of low-temperature modification of  $\text{Ca}_2\text{GeO}_4$  has to be carried out in a temperature range which does not exceed the phase transformation temperature.

This paper describes the development of flux growth technique to produce large crystals of  $\text{Cr}^{4+} : \text{Ca}_2\text{GeO}_4$ , called cunyite.

## 2. Experimental procedure and results

### 2.1. Spontaneous crystallization

It has been reported [7] that small  $\text{Ca}_2\text{GeO}_4$  crystals with a size of up to 1 mm have been grown from the flux based on  $\text{CaCl}_2$  solvent with a  $\text{Ca}_2\text{GeO}_4$  concentration of 50 wt% by conventional slow cooling procedure from 1250°C at a rate of 5°C/h. The main advantage of this solvent is that it does not add unfavorable additional cations into the system. Although this flux exhibits high vapor pressure in a temperature range exceeding 1000°C, our first attempt at growth of  $\text{Ca}_2\text{GeO}_4$  single crystals was done from similar flux based on  $\text{CaCl}_2$ - $\text{CaF}_2$  eutectic mixture (0.2 mol%  $\text{CaF}_2$  and 0.8 mol%  $\text{CaCl}_2$ ) which is

expected to lead to decreasing flux vapor pressure and extending  $\text{Ca}_2\text{GeO}_4$  crystallization field to low-temperature range compared with the system based on  $\text{CaCl}_2$  solvent.

Phase equilibria study and growth of  $\text{Ca}_2\text{GeO}_4$  crystals by conventional slow cooling technique were carried out in a muffle furnace (Thermolyne 4000) in air atmosphere. Pt-crucible (5.08 cm  $\times$  5.08 cm) filled by initial charge was placed into a furnace on alumina pedestal providing strong axial temperature gradient in a melt with overheated crucible bottom. This kind of temperature distribution in a melt created thermal conditions with a first crystal formation occurring on the melt surface. Saturation temperature data were obtained by direct visual observation of initial spontaneous crystallization on the melt surface through a top vertical hole in a muffle furnace. This way, solubility of  $\text{Ca}_2\text{GeO}_4$  in  $\text{CaCl}_2$ - $\text{CaF}_2$  eutectic mixture was estimated to be changed from 35 wt% at 950°C up to 40 wt% at 1050°C. A congruent character of solubility of  $\text{Ca}_2\text{GeO}_4$  was observed in a wide temperature interval (1050–700°C). There are no additional phases found in this temperature range of crystallization.

Spontaneously formed, green color, well-shaped  $\text{Cr} : \text{Ca}_2\text{GeO}_4$  crystals with a size up to  $5 \times 5 \times 10 \text{ mm}^3$  were grown from the solution (35 wt%  $\text{Ca}_2\text{GeO}_4$ ) in a platinum crucible by slow cooling technique. The homogenization temperature of solution was of  $\sim 1050^\circ\text{C}$ , cooling rate — 0.5–2.0°C/h, and temperature range of crystallization — 950–700°C. The starting charges were prepared from a mixture of  $\text{CaCO}_3$ ,  $\text{GeO}_2$ ,  $\text{CaF}_2$ , and  $\text{CaCl}_2$ . Chromium (3+) oxide was added in the system as doped impurity (0.5 wt% relative to  $\text{Ca}_2\text{GeO}_4$ ). Crystals grown were separated from a melt by dissolution of flux medium in hot water. The habit of crystals (Fig. 1) was formed by a combination of the side pinacoid (0 1 0), first-order prism (0 1 1) and rhombic dipyrmaid (1 1 1). Anisotropy of growth rate is strongly displayed at increasing cooling rate up to 5–10°C/h. Occasionally elongated  $\text{Ca}_2\text{GeO}_4$  crystals more than 2 cm long in [1 0 0] direction have been grown during short growth period not exceeding 2 days. Traditional flux inclusions often occurred in spontaneously grown crystals as a consequence of

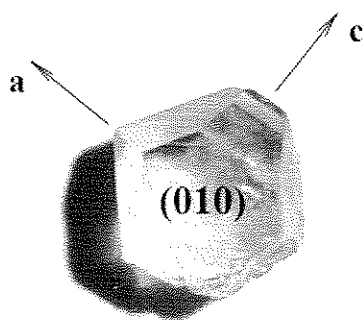


Fig. 1. Typical shape of  $\text{Ca}_2\text{GeO}_4$  crystals grown by spontaneous crystallization from flux.

unstable layered growth. The hygroscopic inclusions attracting water from environment atmosphere were the main reason of strong mechanical stress causing the crystals to crack.

Crystallization from flux by conventional slow cooling technique is known to be very limited and usually considered as only a first step in the development of top-seeding solution growth (TSSG) process. The  $\text{Cr}:\text{Ca}_2\text{GeO}_4$  crystals grown by spontaneous crystallization were only used for preliminary absorption and luminescence measurements and as oriented seeds in TSSG experiments.

## 2.2. Top-seeding solution growth (pulling technique)

The development of pulling technique for  $\text{Cr}:\text{Ca}_2\text{GeO}_4$  solution growth was based on using high-temperature gradient growth conditions to speed up the stable growth rate of crystals. High-temperature gradient normal to the growth interface would be expected to have a stabilizing influence and allow an increasing growth rate without breakdown to cellular growth. RF-heating Czochralski growth apparatus produced by Thermal Technology Inc. was employed for the development of the pulling technique. Calcium chloride has been excluded from solution due to high volatility at elevated temperatures, and only  $\text{CaF}_2$ -based flux was used for growth experiments. Estimated data

on a temperature dependence of  $\text{Ca}_2\text{GeO}_4$  solubility in  $\text{CaF}_2$ -solvent obtained from direct crystal growth experiments are represented in Fig. 2. The saturation temperature was measured by pyrometer while first evidence of crystallization on a seed appeared. This solution as well as Cl-contained one is characterized by congruent solubility of  $\text{Ca}_2\text{GeO}_4$ . Since the temperature interval of crystallization exceeding  $1300^\circ\text{C}$  is usually considered as maximum level for platinum crucible under RF-heating conditions, an iridium crucible, 5.08 cm diameter  $\times$  5.08 cm high, with 2.0 mm thick wall and bottom, and nitrogen atmosphere were chosen for  $\text{Cr}:\text{Ca}_2\text{GeO}_4$  growth procedure. The 15 wt%  $\text{GeO}_2$  excess in respect of  $\text{Ca}_2\text{GeO}_4$  stoichiometry was found to lead to a primary crystallization of  $\text{Ca}_3\text{Ge}_2\text{O}_7$  phase. Cr-doped  $\text{Ca}_3\text{Ge}_2\text{O}_7$  needle-like crystals formed on a melt surface after solidification of  $\text{GeO}_2$ -rich solution was characterized by specific dark-blue color different from blue-green color of  $\text{Cr}:\text{Ca}_2\text{GeO}_4$  crystals.

To determine the optimal temperature-concentration range for crystallization of  $\text{Cr}:\text{Ca}_2\text{GeO}_4$  by pulling technique, numerous probe growth runs have been carried out with different concentration of solution varying from 60 up to 80 wt%  $\text{Ca}_2\text{GeO}_4$ . It was shown that  $\text{CaF}_2$ -based solution with approximate  $\text{Ca}_2\text{GeO}_4$  concentration of 70 wt% and with corresponding saturation

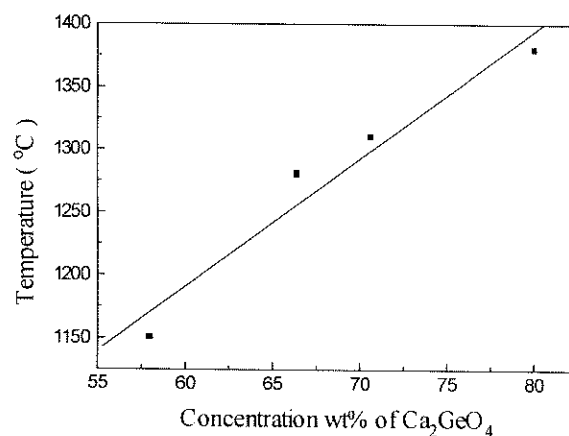
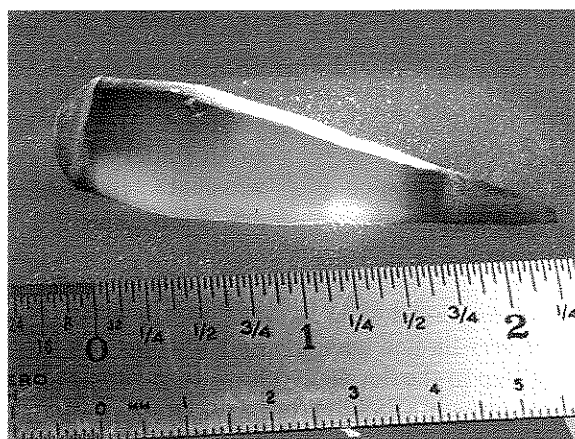


Fig. 2. Temperature dependence of  $\text{Ca}_2\text{GeO}_4$  solubility in  $\text{CaF}_2$ -based solution.

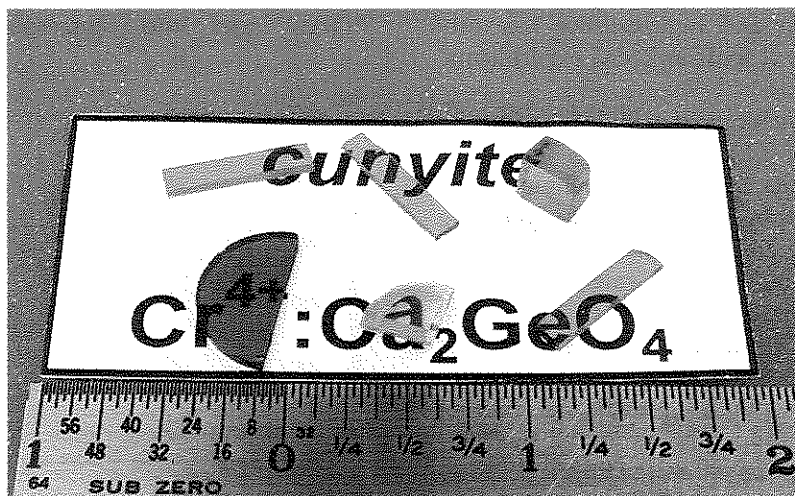
temperature of  $\sim 1350^\circ\text{C}$  provided stable growth conditions during two week long growth runs. Increasing crystallization temperature was shown to lead to considerable losses of flux by evaporation and to unfavorable changes of flux composition. White powder deposited on walls of chamber exhibited hygroscopic properties and attracted water from atmosphere after opening the chamber at the end of run. X-ray powder diffraction analysis of compound deposited on chamber walls showed the presence of  $\text{CaF}_2$  and other unknown phases, one of which being probably  $\text{CaGeF}_6 \times 2\text{H}_2\text{O}$  (after

attracting water from air atmosphere). Total loss of material by evaporation during two week long growth process in  $1350\text{--}1300^\circ\text{C}$  temperature range is estimated to be approximately 5 wt%.

Successful growth experiments by pulling technique have been carried out from  $\text{CaF}_2$ -based flux with  $\text{Ca}_2\text{GeO}_4$  concentration of  $\sim 70$  wt%. The  $\text{Cr}_2\text{O}_3$ -concentration in initial charge was varied from 0.05 up to 0.5 wt%. The parameters of crystallization used are listed below: growth direction —  $[1\ 0\ 0]$ , temperature range —  $1350\text{--}1300^\circ\text{C}$ , pulling rate —  $0.2\text{--}0.1$  mm/h, seed rotation speed



(a)



(b)

Fig. 3.  $\text{Cr}^{4+}:\text{Ca}_2\text{GeO}_4$  crystal grown by pulling technique from flux: (a) as grown; (b) oriented samples for spectroscopic and laser measurements.

— 60 — 20 rpm, growth atmosphere — nitrogen. Fully transparent, dark-green  $\text{Cr}:\text{Ca}_2\text{GeO}_4$  crystals more than 15 mm in diameter and up to 60 mm long have been grown under the above mentioned growth conditions (Fig. 3a). After the growth, slices 2–5 mm thick were cut and hand polished for spectroscopic and laser experiments (Fig. 3b).

### 2.3. Crystal characterization

One of the features of the  $\text{Ca}_2\text{GeO}_4$  grown by pulling technique is that boules never exhibited any facets usually associated with solution growth. Liquid–solid growth interface as well as external surface of crystal was smooth and without facets. The shape of the interface was always convex (Fig. 4). The shape of growth interface is known to reflect a temperature isotherm, character of convection and mechanism of crystallization. All these parameters are supposed to be close to those usually taking place for conventional pulling process from a melt. The main problem of  $\text{Ca}_2\text{GeO}_4$  solution growth by pulling technique was the tendency toward interface breakdown to a cellular structure which usually began at the center of growth interface and spread to the edges as growth proceeded (Fig. 5). Cellular growth was often observed when uncontrolled changes of crystal diameter occurred. We were able to avoid unstable growth conditions by adjusting axial temperature distribution and pulling rate.



Fig. 4. Liquid–solid growth interface.

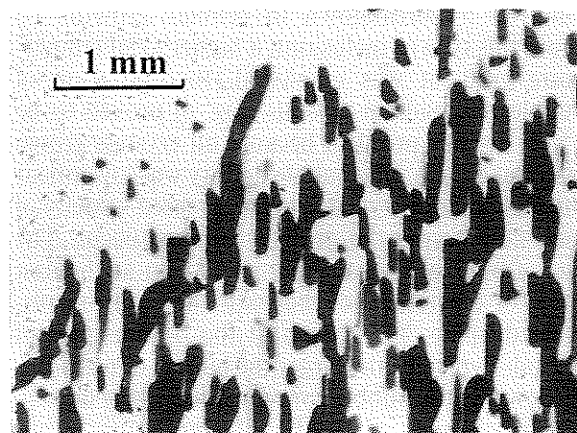


Fig. 5. Unstable growth conditions (inclusion incorporation followed by breakdown to cellular growth).

The high-temperature gradient at the growth interface is known to cause strong residual stresses and crystals readily crack when pulled up from hot to cold zone as well as when cooling down to room temperature after completing growth procedure. Crack formation and propagation strongly depended on the quality of  $\text{Ca}_2\text{GeO}_4$  crystals. Large crystals without cellular growth and other macroscopic defects seldom showed signs of cracking even when cooled down at the rate of 20–50°C/h. If a polycrystalline region formed on a seed at initial stage of crystallization or significant quantity of solution adhered to the bottom of crystal, localized cracking would occasionally occur. Some of the crystals exhibited a vertical crack after cooling down to room temperature, evidence of cleavage in this material. In accordance with X-ray diffraction data,  $\text{Ca}_2\text{GeO}_4$  crystals cleaved perpendicularly to the “*c*”-axis and cleavage plane corresponds to (0 0 1) type of crystallographic planes.

Most  $\text{Ca}_2\text{GeO}_4$  crystals grown contained internal defects which were characterized using optical microscopy. The predominant types of defects found were flux inclusions and bubbles. Discrete flux inclusions incorporation with typical dimensions in the 100–500  $\mu\text{m}$  range were formed in the core region and then extended to the perimeter of crystal. Incorporation of these inclusions was the first evidence of interface instability usually

followed by breakdown to cellular growth. To avoid this type of inclusions, a higher axial temperature gradient was employed. Incorporation of bubbles or voids in crystals (Fig. 6) proved to be a very serious problem because all crystals grown contained them. The bubble density was lower near the perimeter of crystal, where increased velocity of melt flow across the growth interface occur. The size of bubbles was around 50–100  $\mu\text{m}$  at the first stage of crystallization beneath the seed and increased up to 300–500  $\mu\text{m}$  at the bottom part of crystal. Typically, the larger the bubble dimensions, the lower is the bubble concentration in the crystal. The mechanism of the bubble formation is not known with certainty. One possibility includes interface evolution of dissolved gas at growth interface followed by incorporation into crystal.

The  $\text{Cr}_2\text{O}_3$ -concentration in initial charge was varied from 0.05 to 0.5 wt%. Total Cr-concentration in crystals was not known. The crystals grown by pulling technique exhibited much higher density of green color compared with those grown by spontaneous crystallization (at the similar concentration of  $\text{Cr}_2\text{O}_3$  in both systems). We had approximately fivefold increase of absorption coefficient for the first kind of crystals. This increasing Cr-concentration led to considerable change of  $\text{Ca}_2\text{GeO}_4$  unit cell parameters measured by X-ray powder diffraction method ( $a = 5.25 \text{ \AA}$ ,  $b = 11.39 \text{ \AA}$ ,  $c = 6.78 \text{ \AA}$  — for the crystals grown by conventional spontaneous crystallization;  $a = 5.26 \text{ \AA}$ ,  $b = 11.43 \text{ \AA}$ ,  $c = 6.80 \text{ \AA}$  — for the crystals grown by pulling

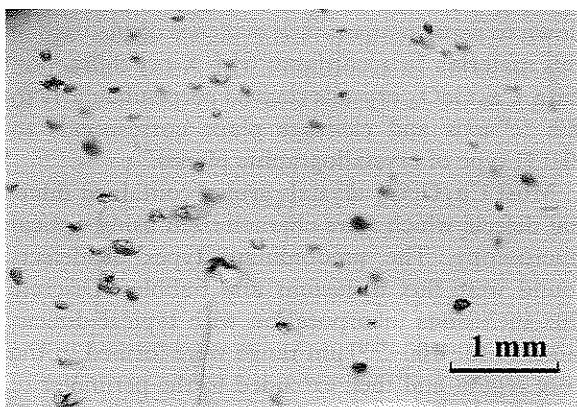


Fig. 6. Bubbles in  $\text{Ca}_2\text{GeO}_4$  crystal.

technique; concentration of  $\text{Cr}_2\text{O}_3$  in the initial charge of both systems was  $\sim 0.5 \text{ wt\%}$ ). The absorption spectra of  $\text{Cr} : \text{Ca}_2\text{GeO}_4$  crystals for three different crystallographic orientations, presented in Fig. 7, show features that are similar to those observed in the absorption spectra of Cr-doped forsterite, the only difference being a significant red shift. The absorption bands observed in the spectra are attributed exclusively to transitions of the  $\text{Cr}^{4+}$  ion. There are no differences observed between the spectra of highly doped  $\text{Cr} : \text{Ca}_2\text{GeO}_4$  prepared by pulling technique and low-doped crystals grown by spontaneous crystallization except an approximately fivefold increase of absorption coefficient. The oxidation state +4 for chromium ion in  $\text{Cr} : \text{Ca}_2\text{GeO}_4$  crystals is very stable and does not depend on growth atmosphere ( $\text{N}_2$  or air).

The emission spectra, shown in Fig. 8, of  $\text{Cr} : \text{Ca}_2\text{GeO}_4$  were measured for 670 nm excitation at room temperature and at liquid  $-\text{N}_2$  temperature. The single band with a maximum at 1290 nm in the room-temperature emission spectrum is attributed to  $\text{Cr}^{4+}$ , indicating that the crystal structure of  $\text{Ca}_2\text{GeO}_4$  allows only the  $\text{Cr}^{4+}$  substitution to take place. There is no  $\text{Cr}^{3+}$  spectral signature. The low-temperature emission spectrum of  $\text{Cr} : \text{Ca}_2\text{GeO}_4$  is characterized by a sharp zero-phonon line at 1200 nm followed by a vibrational sideband similar to the low-temperature spectrum of Cr-forsterite. The fluorescence lifetime of  $\text{Cr}^{4+}$  in  $\text{Ca}_2\text{GeO}_4$  for 1064 nm excitation

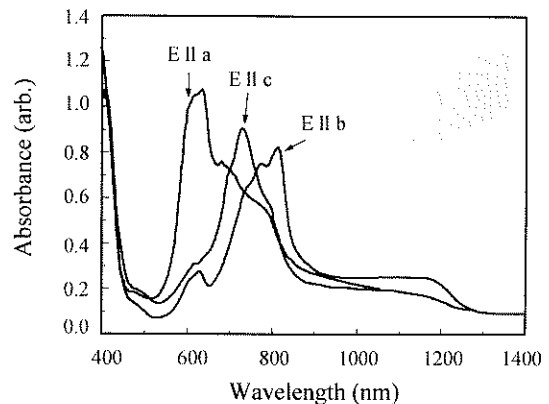


Fig. 7. Polarized absorption spectra of  $\text{Cr}^{4+} : \text{Ca}_2\text{GeO}_4$  crystals.

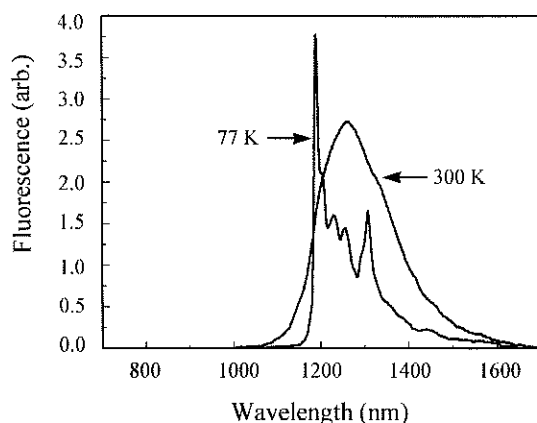


Fig. 8. Emission spectra of  $\text{Cr}^{4+} : \text{Ca}_2\text{GeO}_4$  crystals at 300 and 77 K excited at 670 nm.

is  $\sim 5 \mu\text{s}$  at room temperature for highly doped crystal and  $15 \mu\text{s}$  for low doped one.

The 2–5 mm thick slices cut from boules grown by pulling technique were used for laser experiments. We have recently reported successful tunable laser operation for  $\text{Cr}^{4+} : \text{Ca}_2\text{GeO}_4$  over the 1348–1482 nm spectral range [9,10].

### 3. Summary

The high-quality Cr-doped  $\text{Ca}_2\text{GeO}_4$  crystals suitable for laser applications have been successfully grown in RF-heating pulling equipment designed for conventional Czochralski growth from a melt. Only the  $\text{Cr}^{4+}$ -substitution takes place in Cr-doped  $\text{Ca}_2\text{GeO}_4$  single crystals although nitrogen atmosphere was used in growth process. High concentration of active ions can easily be achieved

in  $\text{Cr}^{4+} : \text{Ca}_2\text{GeO}_4$  crystals. This crystal may represent a laser material suitable for diode pumping and fabrication of miniature laser devices such as microchip and waveguide lasers.

### Acknowledgements

This research was supported by NASA IRA, and New York State Technology Foundation.

### References

- [1] V. Petricevic, S.K. Gayen, R.R. Alfano, *Appl. Phys. Lett.* 53 (1988) 2590.
- [2] A.P. Shkadarevich, in: M.L. Shand, H.P. Jenssen (Eds.), *OSA Proceedings on Tunable Solid State Lasers*, Vol. 5, Optical Society of America, Washington, DC, 1989, pp. 60–65.
- [3] J. Koetke, S. Kuck, K. Petermann, G. Huber, G. Gerullo, M. Danailov, V. Magni, L.F. Qian, O. Svelto, *Opt. Commun.* 101 (1993) 195.
- [4] S. Kuck, K. Peterman, U. Pohlmann, U. Schonhoff, G. Huber, *Appl. Phys. B* 58 (1994) 153.
- [5] V. Petricevic, A. Seas, R.R. Alfano, M.R. Kokta, M.H. Randles, in: *Compact Blue-Green Lasers*, OSA Technical Digest Series, Vol. 2, Optical Society of America, Washington, DC, 1993, pp. 238–240.
- [6] Li Yang, V. Petricevic, R.R. Alfano, in: J.F. Becker, A.C. Tam, J.B. Gruber, L. Lam (Eds.), *Novel Laser Sources and Applications*, SPIE Optical, Engineering Press, Bellingham, Wash, 1994, pp. 103–115.
- [7] M.F. Hazenkamp, U. Oetliker, H.U. Gudel, U. Kesper, D. Reinen, *Chem. Phys. Lett.* 233 (1995) 466.
- [8] A.K. Shirvinskaya, R.G. Grebenshchikov, N.A. Toropov, *Izv. Akad. Nauk SSSR Neorg. Mater.* 2 (1966) 332.
- [9] V. Petricevic, A.B. Bykov, J.M. Evans, R.R. Alfano, *Opt. Lett.* 21 (1996) 1750.
- [10] J.M. Evans, V. Petricevic, A.B. Bykov, A. Delgado, R.R. Alfano, *Opt. Lett.* 22 (15) (1997) 1171.